Measurement of the Two-Halo Neutron Transfer Reaction ^{1}H(^{11}Li, ^{9}Li)^{3}H at 3A MeV

I. Tanihata,* M. Alcorta,† D. Bandyopadhyay, R. Bieri, L. Buchmann, B. Davids, N. Galinski, D. Howell, W. Mills, S. Mythili, R. Openshaw, E. Padilla-Rodal, G. Ruprecht, G. Sheffer, A. C. Shotter, M. Trinczek, and P. Walden
TRIUMF, 4004 Wesbrook Mall, Vancouver, BC, V6T 2A3, Canada

H. Savajols, T. Roger, M. Caamano, W. Mittig,‡ and P. Roussel-Chomaz
GANIL, Bd Henri Becquerel, BP 55027, 14076 Caen Cedex 05, France

R. Kanungo and A. Gallant
Saint Mary's University, 923 Robie St., Halifax, Nova Scotia B3H 3C3, Canada

M. Notani and G. Savard
ANL, 9700 S. Cass Ave., Argonne, Illinois 60439, USA

I. J. Thompson
LLNL, L-414, P.O. Box 808, Livermore, California 94551, USA
(Received 22 January 2008; published 14 May 2008)

The p(^{11}Li, ^{9}Li)t reaction has been studied for the first time at an incident energy of 3A MeV at the new ISAC-2 facility at TRIUMF. An active target detector MAYA, built at GANIL, was used for the measurement. The differential cross sections have been determined for transitions to the ^{9}Li ground and first excited states in a wide range of scattering angles. Multistep transfer calculations using different ^{11}Li model wave functions show that wave functions with strong correlations between the halo neutrons are the most successful in reproducing the observation.

DOI: 10.1103/PhysRevLett.100.192502 PACS numbers: 25.40.Hs, 24.10.Eq, 25.60.Je, 27.20.+n

A neutron halo is a long tail of neutron density distribution in a nucleus extending far beyond that of the tightly bound nucleons. It is formed in an extremely loosely bound nucleus near the limit of existence of bound nuclei. For example, the evidence suggests that the unstable nucleus ^{11}Li exhibits a two-neutron halo structure around a central ^{9}Li core and the distribution of halo neutrons extends to the size of a nucleus with mass number 200. Such wave function has a considerable amplitude in the classically forbidden region and is therefore expected to show interesting quantum effects [1]. Since ^{11}Li is believed to have the most pronounced two-neutron halo, much current research is concentrated on this isotope. Presently the most important question about the halo structure concerns the nature of the interaction and correlation between the two halo neutrons. In a halo, the correlation may be different from that of a pair of neutrons in normal nuclei for several reasons. Halo neutrons are very weakly bound and, therefore, the effect of the continuum becomes important. The wave function of the halo neutrons has an extremely small overlap with that of the protons and they may experience interactions much different from those of neutrons in normal nuclei. The density of halo neutrons is very low compared with normal nuclear density and, thus, may give rise to quite different correlations from those in stable or near-stable nuclei.

So far, there have been a few experimental attempts to elucidate the nature of these correlations between the halo neutrons in ^{11}Li. Zinser *et al.* [2] studied high-energy stripping reactions of ^{11}Li and ^{11}Be to ^{10}Li, and the analyses of the momentum distributions suggests the necessity of considerable mixing of $(1s_{1/2})^2$ and $(0p_{1/2})^2$ configurations in the ground state of ^{11}Li. Simon *et al.* [3] also reported a similar conclusion by another fragmentation experiment of ^{11}Li. The importance of the s-wave contribution is also seen in Coulomb dissociation measurements [4,5]. Determinations of such amplitudes have also been attempted from data associated with the beta-decay of ^{11}Li. However, no definite conclusions could be reached.

The newly constructed ISAC-2 accelerator at TRIUMF now provides the highest intensity beam of low-energy ^{11}Li up to 55 MeV. This beam enabled the measurement of the two-neutron transfer reaction of ^{11}Li for the first time. The reaction Q value of ^{11}Li$(p, t)^9$Li is very large (8.2 MeV) and, thus, the reaction channel is open at such low energies. The beam energy used in this experiment (33 MeV) is not as high as is usually used in studies of direct reactions; nevertheless due to the low separation energy of the two halo neutrons (~400 keV compared with about 10 MeV in stable nuclei) and low Coulomb barrier (~0.5 MeV) the reaction is expected to be mainly direct. Momentum matching is also good at this low energy

because of the small internal momentum of the halo neutrons.

The beam of ^{11}Li was accelerated to an energy of 36.9 MeV. The beam intensity on the target was about 2500 pps on average, and about 5000 pps at maximum. Measurement of the transfer reaction was made possible at this low beam intensity through the use of the MAYA active target detector brought to TRIUMF from GANIL. MAYA has a target-gas detection volume (28 cm long in the beam direction, 25 cm wide, and 20 cm high) for three-dimensional tracking of charged particles, and a detector telescope array at the end of the chamber. Each detector telescope consisted of a 700 μm thick Si detector and a 1 cm thick CsI scintillation counter of 5×5 cm^2. The array consists of 20 telescopes. MAYA was operated with isobutane gas, first at a gas pressure of 137.4 mbar and then at 91.6 mbar. These two different pressure settings were used to cross check the validity of the analysis by changing the drift speed of ionized electrons and by changing the energy loss density. The coverage of center of mass angles was also different at these pressures—as will be discussed later. Reaction events were identified by a coincidence between a parallel plate avalanche chamber (PPAC) placed just upstream of MAYA and the Si array. ^{11}Li ions that did not undergo a reaction were stopped in a blocking material just before the Si array. Details of MAYA can be found in Ref. [6].

The two-neutron transfer reaction $p(^{11}\mathrm{Li}, {}^{9}\mathrm{Li})t$ was identified by two methods depending on the scattering angles. For forward scattering in the c.m., ^{9}Li ions in the laboratory frame are emitted at small angles and have sufficient energies to traverse the gas and hit the Si array, and so ^{9}Li ions were identified by the $\Delta E - E$ method. The ΔE signal was obtained from the last 5 cm of the MAYA gas detector. Tritons emitted near 90 degrees have low energies so that they stop within the gas detector and thus provide total energy signals. However tritons emitted at smaller angles, but larger than the angles covered by the Si array, punch though the gas volume and therefore only scattering angles and partial energy losses in the chamber could be measured. The major background for such events came from the $^{11}\mathrm{Li} + p \rightarrow {}^{10}\mathrm{Li} + d \rightarrow {}^{9}\mathrm{Li} + n + d$ reaction. Fortunately, the kinematical locus of the (p, d) reaction in a two-dimensional plot between emission angles of ^{9}Li and light particles [θ(Li)-θ(light)] is well separated from the punch through (p, t) events.

For large angle scattering in the c.m., tritons were detected by the Si and CsI detectors and identified clearly by the $\Delta E - E$ technique. Under this condition, ^{9}Li stops inside the gas detector volume and thus the total energy, the range, and the scattering angle were determined. Lithium ions can easily be identified from their energy loss along the track, but identification of the isotope mass number is more difficult. The largest number of background events are due to accidental coincidences of scattered ^{11}Li that have higher energies and will hit the Si array. So rejection of such ^{11}Li events was easily accomplished. Use again was made of a θ(Li)-θ(light) correlation plot for final identification of the (p, t) reaction. To remove other sources of background, preselections were applied based on the kinematical constraints of the events using the measured energies in the Si array, the total charges collected in the gas region, and the scattering angles of both particles. The preselections were applied to the ground state and to the first excited state transitions separately. Those selections were set to be wide enough so that the real events would not be lost.

Figure 1(a) shows the θ(Li) vs θ(light) scatter plot after the preselections. Data of both selections are overlaid in the plot. Two clear kinematical loci are seen. The reaction Q value spectra calculated from those angles are shown in the panel (b). The spectra are shown separately for the two preselections, the selection for the ground state of ^{9}Li and the first excited state ^{9}Li (2.69 MeV). Mixing of the ground state transition into the first excited state spectrum is seen in the plot but, can easily be removed by the selection of the Q values. The separation of the ground state and the excited state transition was not clear for the backward scattering. We assumed that all the events are from ground

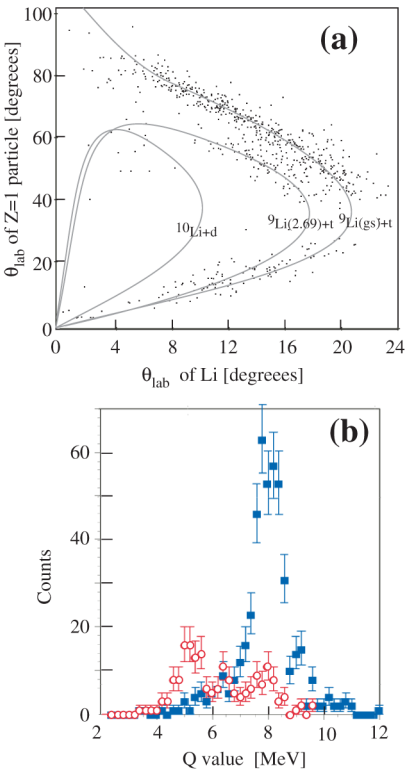

FIG. 1 (color online). (a) θ(Li)-$\theta(H)$ plot. Loci of (p, t) and (p, d) are shown by thin curves. The (p, t) reaction events to the ground and the first excited states are clearly seen. (b) Q-value histograms of (p, t) reactions. Solid squares show the spectrum for ^{9}Li when preselections are for the ground state, and open circles are for events preselected for the first excited state of ^{9}Li.

state transitions for the following analysis. The backward cross section for the ground state therefore may include some component of excited state transitions.

The tracking efficiency was determined by comparing the number of identified particles (by the $\Delta E - E$ method) and the number of tracks that hit an array detector at a consistent position; this comparison was undertaken separately for Li and triton ions. The efficiency of Li tracking was more than 95% and stable from run to run. However the efficiency of triton tracking depends strongly on the energy of the triton and was as low as 70% fluctuating from run to run. Therefore we took this $\pm 10\%$ fluctuation as the uncertainty of the tracking efficiency. The geometrical efficiency was estimated by a Monte Carlo simulation that includes detector geometries and energy losses of the charged particles in the gas.

The number of incident ^{11}Li ions was determined by counting the incident ions both by the PPAC and signals from the first 7 cm of the gas detector. The position, direction, and energy loss along the track of an incident particle were used to select good incident ^{11}Li ions. The uncertainty of the incident beam intensity is $<1\%$. The largest uncertainty in the absolute value of the cross section comes from the uncertainty of tracking efficiency.

Figure 2(a) shows the determined differential cross sections of ground state transitions from the measurements with gas pressure equivalent to 137.4 mbar and 91.6 mbar at 0 °C. The center of mass scattering angles were calculated from the scattering angles of ^{9}Li and the triton. The detection efficiencies are shown in panel (b), as a function of the center of mass angle. At 137.4 mbar, the detection efficiency drops to zero near $\theta_{\rm cm} = 110°$; this is because neither the ^{9}Li nor the triton could reach the array detector. The efficiency of event detection near $\theta_{\rm cm} = 110°$ was higher for the 91.6 mbar setting; under this condition, either the ^{9}Li ion or the triton will hit the array detector for all scattering angles.

For any particular ^{11}Li reaction event, the incident energy depends on the depth of the reaction point within the gas. In the present experiment cross sections were averaged over ^{11}Li energies from 2.8A to 3.2A MeV. The deduced differential cross sections corresponding to the two different pressure settings were consistent within experimental uncertainties. The averaged differential cross sections for transitions to the ^{9}Li ground state are shown in Fig. 3, where the error bars on the figure include only statistical errors. Obviously the data from 105° to 120° were taken only in the 91.6 mbar measurement. In addition to the error bars in the figure, the overall systematic uncertainty of about $\pm 10\%$ should be noted.

The cross section for transitions to the first excited state (Ex = 2.69 MeV) is shown also in Fig. 3. If this state were populated by a direct transfer, it would indicate that a 1^+ or 2^+ halo component is present in the ground state of $^{11}\mathrm{Li}(\frac{3}{2}^-)$, because the spin-parity of the ^{9}Li first excited state is $\frac{1}{2}^-$. This is new information that has not yet been observed in any of previous investigations. A compound

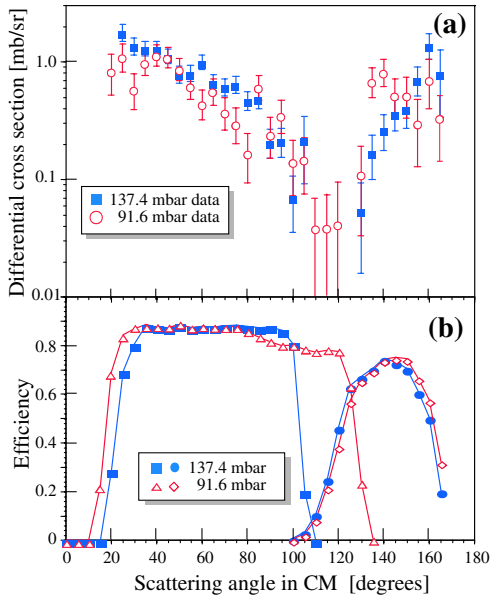

FIG. 2 (color online). (a) The comparison of the differential cross sections for ground state transitions determined from the data sets at 137.4 mbar and 91.6 mbar. (b) The corresponding detection efficiency for each data set. Squares and triangles are for ^{9}Li detection in the Si array, and circles and diamonds are for triton detection events in the Si array. The efficiencies are similar for ground and excited state transitions.

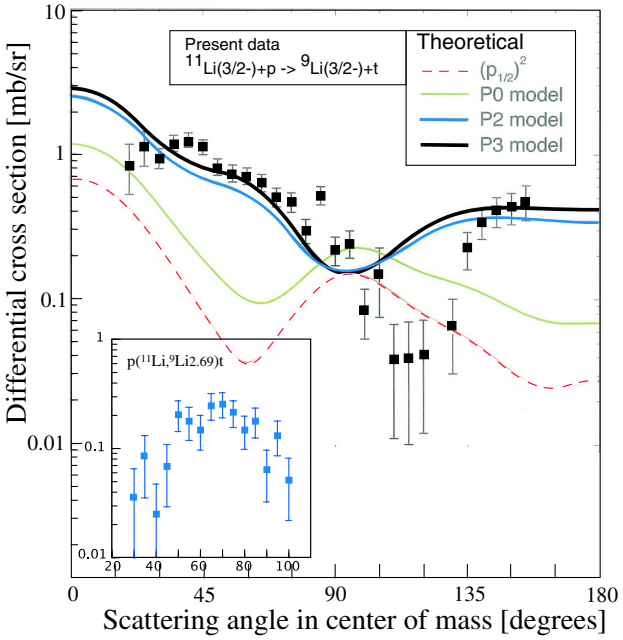

FIG. 3 (color online). Differential cross sections of the (p, t) reaction to the ground state of ^{9}Li and to the first excited state (insert). Theoretical predictions using four different wave functions were shown by curves. See the text for the difference of the wave functions.

TABLE I. Optical potential parameters used for the present calculations.

	V MeV	r_V fm	a_V fm	W MeV	W_D MeV	r_W fm	a_W fm	V_{so} MeV	r_{so} fm	a_{so} fm
$p + {}^{11}$Li [10]	54.06	1.17	0.75	2.37	16.87	1.32	0.82	6.2	1.01	0.75
$d + {}^{10}$Li [11]	85.8	1.17	0.76	1.117	11.863	1.325	0.731	0		
$t + {}^{9}$Li [12]	1.42	1.16	0.78	28.2	0	1.88	0.61	0		

nucleus contribution should be small at the present energy, and in addition the angular distribution of compound decay should be essentially isotropic; hence the deep minimum and the peak observed in the angular distributions of the ground state and the first excited state indicate a limited compound nucleus contribution. However, before a final conclusion as to the reaction mechanism can be made, detailed studies of coupled channels and sequential transfer effects need to be undertaken.

Multistep transfer calculations to determine the differential cross sections to the ground state of ^{9}Li have been made. For these calculations several of the three-body models from Ref. [7], recalculated using the hyperspherical harmonic expansions of Ref. [8], with projection operators to remove the $0s_{1/2}$ and $0p_{3/2}$ Pauli blocked states, have been used. In particular, the $P0$, $P2$ and $P3$ models from [7], which have $(1s_{1/2})^2$ components of 3%, 31%, and 45%, respectively, were used. The corresponding matter radii for ^{11}Li are 3.05, 3.39, and 3.64 fm. For comparison, a simple $(p_{1/2})^2$ model based on the P0 case, but with no n-n potential to correlate the neutrons, was also investigated. All models used here do not include ^{9}Li core excitations.

The calculations reported here include the simultaneous transfer of two neutrons from ^{11}Li to ^{9}Li in a one step process, as well as coherently the two-step sequential transfers via ^{10}Li. The simultaneous transfers used a triton wave fuction calculated in the hyperspherical framework with the SSC(C) nucleon-nucleon force [9], and a three-body force to obtain the correct triton binding energy. The sequential transfers passed through both $\frac{1}{2}^+$ and $\frac{1}{2}^-$ neutron states of ^{10}Li, with spectroscopic factors given by, respectively, the s- and p-wave occupation probabilities for ^{11}Li models of [7]. The spectroscopic amplitudes for $\langle d|t\rangle$ and $\langle {}^{10}\mathrm{Li}|{}^{11}\mathrm{Li}\rangle$ include a factor of $\sqrt{2}$ to describe the doubled probability when either one of the two neutrons can be transferred. S and P wave radial states were used with effective binding energies of 1.0 and 0.10 MeV respectively; this ensured a rms radius of $\sim$6 fm, which is the mean n-^{9}Li distance in the ^{11}Li models. The proton, deuteron and triton channel optical potentials used are shown in Table I. The differential cross sections were obtained using FRESCO [13].

The curves in Fig. 3 show the results of the calculations. The wave function $(p_{1/2})^2$ with no n-n correlation gives very small cross sections that are far from the measured values. The $P0$ wave function, with n-n correlation but with a small $(s_{1/2})^2$ mixing amplitude also gives too small cross sections. The results of the $P2$ and $P3$ wave functions fit the forward angle data reasonably well but the fitting near the minimum of the cross section is unsatisfactory. The results may be sensitive to the choice of the optical potentials as well as the selection of the intermediate states for two-step processes. Detailed analysis of such effects should be a subject of future studies.

In summary, we have measured for the first time the differential cross section for a two-halo neutron transfer reaction of the most pronounced halo nucleus ^{11}Li. Transitions were observed to the ground and first excited state of ^{9}Li. Multistep transfer calculations were applied with different wave functions of ^{11}Li. It is seen that wave functions with strong mixing of p and s neutrons which include three-body correlations provide the best fit to the data for the magnitude of the reaction cross section. However the fitting to the angular shape is less satisfactory. The population of the first excited state of ^{9}Li suggests a 1^+ or 2^+ configuration of the halo neutrons. This shows that a two-nucleon transfer reaction as studied here may give a new insight in the halo structure of ^{11}Li. Further studies clearly are necessary to understand the observed cross sections as well as the correlation between the two halo neutrons.

One of the authors, IT, acknowledges the support of TRIUMF throughout his stay at TRIUMF. The experiment was supported by GANIL and technical help from J. F. Libin, P. Gangnant, C. Spitaels, L. Olivier, and G. Lebertre is gratefully acknowledged. This work was supported by the NSERC of Canada through TRIUMF and Saint Mary's University. Part of this work was performed under the auspices of the U.S. Department of Energy by Lawrence Livermore National Laboratory under Contract No. DE-AC52-07NA27344. This experiment was the first experiment at the new ISAC-2 facility. The authors gratefully acknowledge R. Laxdal, M. Marchetto, M. Dombsky and all other staff members at TRIUMF for their excellent effort for setting up the beam line and delivering the high-quality ^{11}Li beam.

*Present address: RCNP, Osaka University, Mihogaoka, Ibaraki 567-0047, Japan.

†Present address: Institute de Estructura de la Materia, CSIC, Serrano 113bis, E-28006 Madrid, Spain.

‡Present address: NSCL, MSU East Lansing, MI 48824-1321, USA.

[1] I. Tanihata, J. Phys. G **22**, 157 (1996).
[2] M. Zinser *et al.*, Nucl. Phys. **A619**, 151 (1997).
[3] H. Simon *et al.*, Phys. Rev. Lett. **83**, 496 (1999).
[4] S. Shimoura *et al.*, Phys. Lett. B **348**, 29 (1995).
[5] T. Nakamura *et al.*, Phys. Rev. Lett. **96**, 252502 (2006).
[6] C. E. Demonchy *et al.*, Nucl. Instrum. Methods Phys. Res., Sect. A **573**, 145 (2007).
[7] I. J. Thompson and M. V. Zhukov, Phys. Rev. C **49**, 1904 (1994).
[8] I. J. Thompson *et al.*, Phys. Rev. C **61**, 024318 (2000).
[9] R. de Tourreil and D. W. L. Sprung, Nucl. Phys. **A242**, 445 (1975).
[10] F. D. Beccehetti and G. W. Greenless, Phys. Rev. **182**, 1190 (1969).
[11] W. W. Daehnick, J. D. Childs, and Z. Vrcelj, Phys. Rev. C **21**, 2253 (1980).
[12] F. D. Becchetti and G. W. Greenlees, Annual Report, J. H. Williams Laboratory, University of Minnesota, 1969.
[13] I. J. Thompson, Comput. Phys. Rep. **7**, 167 (1988).